Pharmaceutical Development and Technology

ISSN: 1083-7450 (Print) 1097-9867 (Online) Journal homepage: http://www.tandfonline.com/loi/iphd20

Preparation and Characterization of Angiopep-2 Functionalized Ginsenoside-Rg3 Loaded Nanoparticles and the Effect on C6 Glioma Cells

Xiaomei Su, Danshen Zhang, Haiwei Zhang, Kaiyan Zhao & Wenshu Hou

To cite this article: Xiaomei Su, Danshen Zhang, Haiwei Zhang, Kaiyan Zhao & Wenshu Hou (2019): Preparation and Characterization of Angiopep-2 Functionalized Ginsenoside-Rg3 Loaded Nanoparticles and the Effect on C6 Glioma Cells, Pharmaceutical Development and Technology, DOI: 10.1080/10837450.2018.1551901

To link to this article: https://doi.org/10.1080/10837450.2018.1551901

Accepted author version posted online: 02 Jan 2019.

Preparation and Characterization of Angiopep-2 Functionalized Ginsenoside-Rg3 Loaded Nanoparticles and the Effect on C6 Glioma Cells

Xiaomei Su[a], Danshen Zhang[a,b]*, Haiwei Zhang[c],

Kaiyan Zhao[b], Wenshu Hou[c]

a. Department of Pharmacology, Hebei Medical University, Shijiazhuang, China.

b. College of Chemical and Pharmaceutical Engineering, Hebei University of Science and Technology, Shijiazhuang, China.

c. Department of Pharmacy, Hebei North University, Zhangjiakou, China.

Xiaomei Su, E-mail address: Suxm2017@126.com

https://orcid.org/0000-0001-9767-2281

*The corresponding author: Danshen Zhang

Phone number: +86-13832309966

E-mail address: zhangds2011@126.com

The number of words in the text is 6453.

Preparation and Characterization of Angiopep-2 Functionalized Ginsenoside-Rg3 Loaded Nanoparticles and the Effect on C6 Glioma Cells

Abstract

The purpose of this work was to prepare and characterize Angiopep-2 functionalized ginsenoside-Rg3 loaded nanoparticles (ANG-Rg3-NP) and evaluate the therapeutic effect on C6 glioma cells. Nanoparticles were prepared by the emulsion solvent evaporation method. Angiopep-2 was functionalized to nanoparticles via a maleimide-thiol covalent binding reaction to obtain ANG-Rg3-NP. The prepared nanoparticles were evaluated for size, zeta potential, morphology, stability, encapsulation efficiency, loading capacity and release properties. The cytotoxicity study and targeting effect of ANG-Rg3-NP were evaluated by MTT assay. The study of cellular uptake in C6 glioma cells was performed by fluorescence microscopy and by using a microplate reader. The prepared ANG-Rg3-NP was observed to be uniformly spherical in shape with a particle size at 147.1±2.7 nm. The encapsulation efficiency and loading capacity reached 80.6±3.0% and 27.2±1.4%, respectively. Additionally, ANG-Rg3-NP exhibited a desirable sustained release behavior. *In vitro* cytotoxicity study indicated that ANG-Rg3-NP could inhibit the proliferation of C6 glioma cells in a concentration-dependent manner. Also, the functionalization of Angiopep-2 made nanoparticles cross the blood-brain barrier more easily and accelerated the cellular uptake of nanoparticles. The ANG-Rg3-NP was a promising brain drug delivery carrier for the treatment of glioma.

Keywords: Ginsenoside-Rg3; Angiopep-2; PCL-PEG;
Nanoparticles; C6 glioma cells

1. Introduction

Glioma is one of the most common and aggressive intracranial malignancies with high morbidity and mortality. The median overall survival of glioma patients is 12-18 months and the 5-year survival rate is less than 10% (Dizon et al. 2016; Li et al.

2016). The glioma is different from other cancers due to its diffuse invasion of the surrounding normal brain tissue, which makes it is impossible to completely remove glioma by conventional surgery (Ong et al. 2009). In one study, chemotherapy was an essential part of auxiliary treatment of glioma, but the result was disappointing due to the blood-brain barrier (Jain et al. 2007). The blood-brain barrier prevents nearly 100% of large-molecule drugs including peptides, recombinant proteins, monoclonal antibodies and approximately 98% of small-molecule drugs from being transported into the brain (Pardridge 2003).

Ginseng is a traditional Chinese drug, with a long medicinal history. The main active components of Ginseng are the ginsenosides, among which the ginsenoside-Rg3 (Rg3) is the protopanaxadiol type of dammarane ginsenoside, has recently emerged as an effective anticancer medicine with evident antitumor effects and no observed toxic adverse reactions (Kim et al. 2015). Some research reported that ginsenoside-Rg3 exhibited an inhibitory effect against human glioblastoma U87MG cells and induced apoptosis, the mechanisms of apoptosis were related with the MEK signaling pathway and reactive oxygen species (Choi et al. 2013). Also, one research group reported that chronic-treatment with 20(S)-Rg3 in a sub-lethal concentration induced senescence-like growth arrest in U87MG cells (Sin et al. 2012). What's more, some research showed that combined use of temozolomide with ginsenoside-Rg3 displayed additive inhibition on proliferation of both human umbilical vein endothelial cells and rat C6 glioma cells *in vitro* (Sun et al. 2016). Unfortunately, the activity of ginsenoside-Rg3 against glioma has been disappointing in clinical study because poor solubility as well as poor blood-brain barrier permeability.

Interest in design and developing nanoparticles for applications in catalyst, optics, electronics and biomedicine has continued to grow in the past decade due to their unique physical and chemical properties (Nomani et al. 2017). Some research presented the synthesis and preliminary drug delivery evaluation of novel magnetic nanoparticles in order to fully exploit their potential as drug delivery system (Nosrati

et al. 2018). Also, one research group reported that synthesized magnetic nanoparticles coated with glycine and studied its cytotoxic effect *in vitro* (Nosrati et al. 2018). Coating and modification of the nanoparticles with various biocompatible and biodegradable materials has been widely studied (Nosrati et al. 2017; Salehiabar et al. 2018). Targeted delivery of drugs encapsulated within nanocarriers can overcome problems exhibited by "free" drugs, including poor solubility, limited stability, rapid clearing and avoid nonspecific toxicity to normal cells due to lack of selectivity (Ashley et al. 2011). It can be concluded that application of nanoparticles can be more effective strategy for controlled and slow release of drugs in human cancer treatment.

In recent years, a number of materials have become more widely used in the pharmaceutical field because of their excellent biodegradability, biocompatibility and mechanical properties (Deng et al. 2012). Among them, poly (ε-caprolactone)-poly (ethylene glycol) copolymers (PCL-PEG) has been approved for human use by the U.S. Food and Drug Administration (Cabral et al. 2014; Lin 2015) and has been widely used in drug delivery system. The drug delivery system based on PEG-PCL can be modified with various ligands to enable their entry into glioma after intravenous administration via receptor-mediated pathways (Beduneau et al. 2007).

Angiopep-2, a Kunitz domain-derived peptide from protease enzyme, is widely used as specific ligand for low-density lipoprotein receptor-related protein-1 (LRP-1). Actually, LRP-1 was found not only to be over-expressed on blood-brain barrier, but also expressed in malignant astrocytomas, especially in glioblastoma or glioma cells (Xin et al. 2012). Hence, LRP-1 would become a crucial target for the brain-targeting approach. Recent studies reported that LRP-1 successfully mediated the uptake of Angiopep-2, resulting in Angiopep-2 cross the blood-brain barrier and accumulated in parenchyma (Demeule et al. 2008).

In this paper, we report on the preparation and physicochemical characterization of Angiopep-2 functionalized ginsenoside-Rg3 loaded nanoparticles (ANG-Rg3-NP) and *in vitro* therapeutic effect on C6 glioma cells. Nanoparticles were chosen as the

delivery vehicle because of the nontoxic and nonimmunogenic characteristics, the high drug loading ability and the possibility to be decorated with different ligands. Also, we selected Angiopep-2 as a model targeting ligand because of its high affinity for LRP-1, Angiopep-2 was functionalized to nanoparticles via a maleimide-thiol covalent binding reaction aiming at achieving the targeted drug delivery system. Ginsenoside-Rg3, as a model drug, was encapsulated in nanoparticles to evaluate its effect on C6 glioma cells. We used brain microvascular endothelial cells (BMEC) as the model of blood-brain barrier and C6 glioma cells as the model of tumor cell to establish the BMEC-C6 cells co-culture model. The ANG-Rg3-NP crossed the blood-brain barrier and accumulated in C6 glioma cells (Figure 2). The anti-tumor efficacy of ANG-Rg3-NP was evaluated in an *in vitro* cytotoxicity study and targeting effect. What's more, the penetration ability of ANG-Rg3-NP was examined by using coumarin-6 as the fluorescence probe.

2. Materials and methods

2.1. Materials

PCL_{10000}-PEG_{2000} and PCL_{12000}-PEG_{2000}-MAL (MMCO=14KDa) were purchased from Xi'an ruixi Biological Technology Co., Ltd (Xi'an, China) and their chemical structures were showed in Figure 1. Angiopep-2 (TFFYGGSRGKRNNFKTEEYC) was obtained from Zhejiang Ontores Biotechnologies Co., Ltd (Zhejiang, China). Ginsenoside-Rg3 was purchased from Sichuan Victory Biological Technology Co., Ltd (Sichuan, China). Sodium cholate hydrate was obtained from Tokyo Chemical Industry (Tokyo, Japan). The MTT and BCA kit were purchased from Beyotime Biotechnology Co., Ltd (Nantong, China). HPLC-grade acetonitrile and methanol were provided by Thermo Fisher Scientific (Waltham, USA). Coumarin-6 was purchased from Sigma-Alderich (St. Louis, MO, USA). 6, 24 and 96-well plates were purchased from Corning Incorporation (New York, USA). Dimethylsulfoxide (DMSO) and 4',6-diamidino-2-phenylindole (DAPI) were purchased from Bioss Antibodies (Beijing, China). 4% formaldehyde and Triton X-100 were provided by Solarbio

(Beijing, China). All the other solvents were analytical grade.

2.2. Cells

Penicillin-streptomycin (PS), fetal bovine serum (FBS), horse serum (HS) and 0.25% (w/v) trypsin solution were purchased from Gibco (Ontario, Canada). The rat C6 glioma cell line was purchased from ScienCell Biotechnology (California, USA) and maintained in F12K medium supplemented with 15% HS, 10% FBS and 1% PS at 37℃ in a humidified atmosphere containing 5% CO_2.

The endothelial cell medium (ECM) and endothelial cell growth supplement (ECGS) were purchased from ScienCell Biotechnology (California, USA). The BMEC was isolation and culture from primary SD rats. The BMEC was cultured in ECM medium supplemented with 5% FBS, 1% ECGS and 1% PS at 37℃ in a humidified atmosphere containing 5% CO_2.

2.3. Preparation of ANG-Rg3-NP

Nanoparticles were prepared by the emulsion solvent evaporation method (Warsi et al. 2014). Briefly, PCL-PEG (contained the weight of PCL-PEG-MAL was 1 mg and the weight of PCL-PEG was 4 mg) were dissolved in dichloromethane (1 mL). Next, ginsenoside-Rg3 (3 mg) was dissolved in methanol (1 mL). Then mixed dichloromethane and methanol as the oil phase (2 mL). The sodium cholate solution (0.5%, 5 mL) was taken as the water phase, and the oil phase was slowly dripped into water phase and then sonicated in iced water bath until the suspension became a white emulsion. The organic solvent was removed by a rotary vacuum evaporator with a vacuum pressure of 0.08 MPa (RE201D, Gongyi, Yingyu High-tech Instrumental Factory, China) at 40℃ to obtain a blue transparent solution. The solution was then filtrated through 0.22 μm membrane to remove the non-incorporated ginsenoside-Rg3 and centrifuged at 10000 rpm for 30 min at 4℃. The precipitation was washed twice with deionized water and dispersed by phosphate-buffered saline (PBS, pH 7.0) to obtain ginsenoside-Rg3 nanoparticles solution (Rg3-NP).

The calculated Angiopep-2 was added to Rg3-NP solution. The suspension was mangetically stirred at room temperature for 12 h away from light. The free Angiopep-2 was removed by high-speed centrifugation (3-30K, Sigma, USA) at 8000 rpm for 15 min. The precipitation was washed twice with deionized water and dispersed by PBS solution (pH 7.0) to obtain Angiopep-2 functionalized ginsenoside-Rg3 loaded nanoparticles (ANG-Rg3-NP) (Xin et al. 2011).

The methods of preparation coumarin-6 nanoparticles (coumarin-6-NP) and Angiopep-2 functionalized coumarin-6 loaded nanoparticles (ANG-coumarin-6-NP) were the same as that of preparation Rg3-NP and ANG-Rg3-NP, except that coumarin-6 of the same weight was added to the nanoparticles instead of ginsenoside-Rg3.

2.4. Characterization of ANG-Rg3-NP

2.4.1. Particle size and zeta potential analysis

The size of ANG-Rg3-NP and Rg3-NP were determined by using a Zetasizer Nano instrument (ZEN3690, Malvern, UK). The prepared nanoparticles were dispered evenly with PBS (pH 7.0) and were determined by using this Zetasizer Nano instrument.

2.4.2. Transmission electronic microscopy (TEM) images of ANG-Rg3-NP

The surface morphology of the ANG-Rg3-NP was imaged by transmission electronic microscopy (TEM, H-7650, Hitachi, Tokyo, Japan) after staining with 2% (w/v) phosphotungstic acid solution and drying at room temperature.

2.4.4. Determination of encapsulation efficiency (EE) and loading capacity (LC)

Added dichloromethane to ANG-Rg3-NP solution and ultrasonic dissolved the nanoparticles. Then added methanol to the suspension and centrifuged at 3000 rpm for 5 min. The EE and LC were obtained by measuring the ultraviolet absorption of

the supernatant via high performance liquid chromatography (HPLC) system (Waters 2695, Milford, USA). The samples were eluted by a Thermo ODS column (5 μm, 4.6 mm×250 mm) at 30℃ and monitored at 203 nm with an injection of 10 μL. The retention time of ginsenoside-Rg3 was about 10 min. The calibration curve was linear in the range of 5-300 μg/mL of ginsenoside-Rg3 dissolved in methanol with a correlation coefficient of R^2=0.9998.

EE and LC were calculated using the following equations:

$$EE\% = \left(\frac{\text{weight of Rg 3 in nanoparticles}}{\text{weight of Rg 3 fed initially}} \right) \times 100$$

$$LC\% = \left(\frac{\text{weight of Rg 3 in nanoparticles}}{\text{weight of polymers} + \text{weight of Rg 3 in nanoparticles}} \right) \times 100$$

2.4.5. Conjugation efficiency (CE) of Angiopep-2

The CE of Angiopep-2 was determined via a BCA protein quantitation kit, a rapid and highly sensitive method for the quantitation of peptides and proteins.

Preparation of calibration curve of the standard protein solution: The bovine serum albumin solution (0.5 mg/mL) in the kit was added to 96-well plates at the volume of 0, 1, 2, 4, 8, 12, 16 and 20 μL, respectively. Then, PBS buffer (pH 7.0) was added to 96-well plates and made the total volume of each well was 20 μL. The BCA reagent were added according to the instructions of the BCA kit, the absorbance of every well was determined by microplate reader (cytation 5, Biotek, Vermont, USA) at 570 nm.

Sample determination: Took ANG-Rg3-NP solution of 20 μL and added some BCA reagent according to the instructions of the BCA kit. Then, measured the absorbance of ANG-Rg3-NP and calculated the concentration of Angiopepe-2 via calibration curve. The calculation formula was as follows (Liu et al. 2013):

$$CE(\%) = \left(\frac{\text{amount of Angiopep-2 conjugated to the nanoparticles surface}}{\text{total amount of Angiopep-2 added}} \right) \times 100$$

2.4.6. Critical micelle concentration

The critical micelle concentration was measured by a fluorescence spectrophotometer (F7000, Hitachi, Tokyo, Japan) and the pyrene was used as a fluorescence probe. The concentration of pyrene in acetone solution remained 6×10^{-7} M. Then, the suspension was placed in a fume cupboard to evaporate the organic solvent. The blank PCL-PEG nanoparticles were added to the suspension at the final concentration of PCL-PEG (0.4, 0.6, 0.8, 1.0, 5, 10, 25, 50, 100 μg/mL), and then sonicated in a water bath at 50℃ for 2 h, stayed at room temperature for 12 h away from light. The fluorescence excitation spectra of the solutions were scanned at 300~360nm with the fixed emission wavelength of 390nm. The slit of excitation and emission was 5.0 nm (Zhu et al. 2016).

2.4.7. Differential scanning calorimetry

The prepared nanoparticles were processed into powder via freeze-dryer. The existing state of ginsenoside-Rg3 in ANG-Rg3-NP was examined by using a differential scanning calorimeter (DSC 1 STAR^e System, Mettler Toledo, Shanghai, China). The parameters of the measurement program as follows: the heating rate was 10℃/min, and the temperature ranging from 30℃ to 450℃. The capped crucible without sample was taken as the control, The curves of ginsenoside-Rg3, Angiopep-2, ANG-NP, ANG-Rg3-NP as well as the physical mixture of ginsenoside-Rg3 and ANG-NP were recorded (Mohammadi et al. 2017).

2.4.8. In vitro release of ANG-Rg3-NP

In vitro Rg3 release profile study was performed by using the dialysis method. Briefly, 4 mL of ginsenoside-Rg3, Rg3-NP and ANG-Rg3-NP were placed into sealed dialysis bags (MWCO=8 kDa) and submerged fully into 200 mL saline with 1% Tween-80 (pH 7.0). In the condition of 37℃ and stirring at 100 rpm for 96 h. At

predetermined time points (1, 2, 3, 4, 6, 8, 12, 24, 48, 72 and 96 h), 2 mL release media was withdrawn and replaced with equal volume of fresh release media. The concentrations of ginsenoside-Rg3 in samples were determined by HPLC analysis as described previously (Hu et al. 2013).

2.4.9. In vitro cytotoxicity study

For drug delivery and other biomedical uses, toxicity is a critical aspect to consider when evaluating their applications. In this study, we selected C6 cells with higher expression of LRP-1 to evaluate the cytotoxicity of nanoparticles *in vitro*. To examine the inhibitory effect on cancer cells, C6 glioma cells were treated with pure Rg3, Rg3-NP and ANG-Rg3-NP suspensions and studied by MTT assay (Salehiabar et al. 2018). Briefly, C6 cells were seeded into 96-well plates at the density of 1×10^4 cells/well. After that, the plates were cultured for 24 h at 37°C. The medium was removed and the cells were washed twice with PBS. Different nanoparticles of Rg3-NP and ANG-Rg3-NP were diluted at the concentration of Rg3 ranging from 0.125, 0.25, 0.375, 0.5, 0.75 to 1.00 mg/mL. Then the nanoparticles were added into each well for 48 h. After treatment, 10 μL MTT solution (5 mg/mL) was added and allowed to incubate for 4 h. Then, the medium was removed and 100 μL dimethylsulfoxide (DMSO) was added, followed by gently shaking to dissolve the formazan crystals. The absorbance was measured via a microplate reader (cytation 5, Biotek, Vermont, USA) at 490 nm. The cells that were not treated with drugs served as the control group, and the well without added cells served as the blank group (Chen et al. 2017). The formula for caclculating the cell inhibition was as follows:

$$\text{cell inhibition (\%)} = 1 - \left(\frac{\text{the absorbance of experimental group} - \text{the absorbance of control group}}{\text{the absorbance of control group} - \text{the absorbance of control group}} \right) \times 100$$

2.4.10. Targeting effect in vitro

The blood-brain barrier is a specialized system of endothelial cells that separates the blood from the underlying brain cells, providing protection of neurons and preserving central nervous system homeostasis (Koo et al. 2006). Angiopep-2 is used

as specific ligand for LRP-1 which was found not only to be over-expressed on BMEC cells, but also expressed in C6 glioma cells. However, in order to enter C6 cells, nanoparticles must pass through BMEC cells. For evaluating the targeting effect of ANG-Rg3-NP *in vitro*, the BMEC-C6 cells co-culture model was established.

The BMEC cells were seeded into 12-transwell plates at the density of 5×10^4 cells/well for 6 days, and the medium was changed every other day. The transepithelial electrical resistance (TEER) of transwell-chambers were measured by Epithelial Volt-Ohm Meter (Millcell® ERS-2, Merck Millipore, USA) and the TEER that larger than 180 cm^2 was selected for the following experiment (Arthur 2000). The C6 cells were seeded into another 12-well plates at the density of 1×10^4 cells/well for 1 day. Then the transwell was inserted into the C6 plates for 1 day to establish the co-cultured model *in vitro* (Figure 3).

After that, the culture medium was removed and the cells were washed twice with PBS. Free ginsenoside-Rg3, Rg3-NP, ANG-Rg3-NP were diluted with medium (free of serum) at the concentration of contained ginsenoside-Rg3 was 200 μg/mL. We set up another group of ANG-Rg3-NP+Angiopep-2, in this group, the concentration of contained ginsenoside-Rg3 was 200 μg/mL and the concentration of free Angiopep-2 was 100 μg/mL. Then, these four groups were added into a transwell for 12 h, respectively. After removal of the transwell, the C6 cells were further cultured for another 48 h and cell inhibition was measured by MTT assay as described previously.

2.4.11. Cellular uptake on C6 cells

Qualitative analysis of cellular uptake of Rg3-NP and ANG-Rg3-NP was performed via fluorescent microscopy, using coumarin-6 as the fluorescent probe. For the experiment, C6 cells were seeded into 24-well plates at the density of 5×10^4 cells/well and cultured at 37°C for 24 h, then checked under the microscope for confluency and morphology. Cells achieving 70-80% confluence were exposed to coumarin-6-loaded PCL-PEG nanoparticles (coumarin-6-NP) and Angiopep-2

functionalized coumarin-6-loaded PCL-PEG nanoparticles (ANG-coumarin-6-NP) in serum-free media for 1 h at the concentration of coumarin-6 ranging from 10 μg/mL to 50 μg/mL. After that, the culture medium was removed and the cells were washed with cold PBS, fixed with 4% (w/v) formaldehyde at room temperature for 15 min away from light, stained with DAPI for 5 min and visualized under a fluorescent microscope (eclipse Ti, Nikon, Tokyo, Japan) (Gu et al. 2013).

For quantitative experiments, C6 cells were seeded in 24-well plates at a density of 5×10^4 cells/well and allowed for attachment for 24 h. Added coumarin-6-NP, ANG-coumarin-6-NP and ANG-coumarin-6-NP+Angopep-2 (10 μg/mL) with the concentration of coumarin-6 ranging from 10 μg/mL to 50 μg/mL into plate. Two hours later, the cells were washed three times with cold PBS. In addition, to study the effect of incubation time on nanoparticles uptake, the cells were incubated with the coumarin-6-NP and ANG-coumarin-6-NP with the concentration of coumarin-6 was 30 μg/ml at 37°C for 0.5, 1, 2, 3 and 4 h, respectively. Then, the cells were washed three times with cold PBS. After washing, C6 cells were lysed with 1% Triton X-100 and centrifuged at 6000 rpm for 5 min. Fluorescence of coumarin-6 in the supernatant was measured by a microplate reader at Ex=467 nm, Em=502 nm. The C6 cells cultured under normal conditions were used as the control.

2.5. Statistical analysis

All data were expressed as mean±standard deviation (SD) and the statistical significance of differences were conducted by by one-way ANOVA using SPSS (IBM SPSS Statistics 19). A P-value (P) less than 0.05 was defined as significant.

3. Results

3.1. Characterization of ANG-Rg3-NP

3.1.1. Particle size and zeta potential analysis

In our study, the size of nanoparticle was increased from 135.6±4.2 nm to

147.1±2.7 nm after modification with Angiopep-2 (Table 1). The mean diameter of Rg3-NP and ANG-Rg3-NP were less than 150 nm, with an acceptably good polydispersity index (PDI<0.15), which was similar to the result of the TEM image (Figure 4). Otherwise, the nanoparticles will get benefit from enhanced permeability and retention (EPR) effect to accumulate in tumor due to the cut-off size of leaky blood vessels which was under 150 nm (Tang et al. 2014).

The zeta potential of Rg3-NP and ANG-Rg3-NP were -28.5±2.5 mV and -14.6±3.2 mV, respectively (Table 1). The negative charge of nanoparticles will inhibit the plasma protein dilution and prolong the circulation time (Li and Huang 2008). Also, the negative surface charge determined nanoparticles have higher dispersion stability and the better interactions with cell membrane via electrostatic repulsion *in vivo* (Liu et al. 2016).

3.1.2. Transmission electronic microscopy (TEM) images of ANG-Rg3-NP

As can be seen from the TEM image (Figure 4), the nanoparticles exhibited spherical shape with uniform size and well-distributed form. The mean diameter of ANG-Rg3-NP was close to 150 nm. which was similar to the result of Zetasizer Nano instrument.

3.1.4. Determination of encapsulation efficiency (EE) and loading capacity (LC)

Compared with Rg3-NP, the EE and LC of ANG-Rg3-NP decreased to some extent (Table 2). It may be due to some ginsenoside-Rg3 released from nanoparticles during the reaction between Angiopep-2 and Rg3-NP.

3.1.5. Conjugation efficiency of Angiopep-2

The calculated conjugation efficiency of Angiopep-2 was 39.51±0.9% in the condition of the molar ratio of PCL-PEG-MAL to Angiopep-2 was 1:1 and the suspension was mangetically stirred for 12 h away from light.

3.1.6. Critical micelle concentration

With the increase of polymer, pyrene was transferred from water medium to the hydrophobic core of the nanoparticle because of the hydrophobic effect and the polarity of the environment changed, so the spectrum of pyrene had a red shift and the largest excitation wavelength shifted from 340 nm to 338 nm. The ratio of fluorescence intensity at 340nm and 338nm was changed after the nanoparticle formed. The fluorescence intensity of 340nm and 338nm were recorded as I_{340} and I_{338}, respectively. The concentration of PCL-PEG solution was plotted on the horizontal axis, against the fluorescence intensity ratio of PCL-PEG solution at 340 nm and 338 nm (I_{340}/I_{338}) on the vertical axis to obtain the curve of CMC.

As shown in Figure 5, the point of slope changed was the CMC of the polymer. The CMC is not only a strong evidence of self-assembly forming micelles, but also an important parameter to evaluate the stability of the blood circulation of nanoparticle in the body. The lower CMC, the harder it was to be diluted and the performance of the nanoparticles was also more stable (Torehilin 2001). The CMC of PCL-PEG nanoparticles was 4.3616 μg/mL, which was much lower than the concentration of PCL-PEG used in the preparation of Rg3-NP (0.71 mg/mL). It made the nanoparticles possess more hydrophobic reservoirs for drugs and with better stability.

3.1.7. Differential scanning calorimetry

Figure 6 illustrates thermograms of pure ginsenoside-Rg3, ANG-NP, ANG-Rg3-NP as well as the mixture of ginsenoside-Rg3 and ANG-NP. In the thermograms, the melting points of ginsenoside-Rg3 was observed at 82.3°C and 94.8°C, the melting points of ANG-NP was observed at 50.9℃. The mixture of ginsenoside-Rg3 and ANG-NP showed exothermic peak at 50.9°C, 82.3°C and 94.8°C, whereas the DSC thermogram of ANG-Rg3-NP exhibited a single exothermic peak at 50.9℃, which is indicative of a physical interaction between copolymer and ginsenoside-Rg3 upon loading of the drug in nanoparticles (Nosrati et al. 2018). It is commonly preferred that the drug in nanoparticles is amorphous, resulting in better

dissolution, absorption and bioavailability.

3.1.8. In vitro release of ANG-Rg3-NP

As showed in Figure 7, the cumulative release of ginsenoside-Rg3 reached 90% within 12 h for crude ginsenoside-Rg3 which indicated the burst release profile. Compared to crude ginsenoside-Rg3, the Rg3-NP and ANG-Rg3-NP showed a significant sustained release *in vitro*. Besides, both Rg3-NP and ANG-Rg3-NP exhibited a similar ginsenoside-Rg3 release behavior. After 96 h of dialysis in saline, the percentage of ginsenoside-Rg3 released from the Rg3-NP and ANG-Rg3-NP was 79.54% and 78.74%, respectively. It indicated that the modification of Angiopep-2 did not change the release behavior of ginsenoside-Rg3.

3.2. In vitro cytotoxicity study

The IC_{50}, the drug concentration at which the growth of 50% of cells was inhibited, was evaluated by curve fitting of the cell viability data (Nosrati et al. 2017). The IC_{50} values of ANG-Rg3-NP at 48 h were 348 μg/mL versus those of free ginsenoside-Rg3 (540 μg/mL) and Rg3-NP (434 μg/mL). The data exhibited that cell toxicity was directly commensurate to Rg3 concentration over a 48 h time period. The toxicity of the ANG-Rg3-NP increased as the increasing concentrations of ANG-Rg3-NP (Figure 8). Compared with pure ginsenoside-Rg3, cells exposed to ANG-Rg3-NP and Rg3-NP, the amount of living cells was obviously decreased, which was attributed to the cytotoxic effect of Rg3 released from the nanoparticles. Also, the ANG-Rg3-NP and Rg3-NP showed a similar reduction in cell viability, the inhibition effect of ANG-Rg3-NP at an equivalent concentration appeared to be more effective. This effect was likely due to higher internalization yields afforded by nanoparticle-mediated drug delivery (Rostamizadeh et al. 2018). Similar results and conclusions have been reported for other drug delivery systems (Benyettou et al. 2017). These results demonstrated that ANG-Rg3-NP increased the inhibition effect of ginsenoside-Rg3 in C6 cell lines and ANG-Rg3-NP have a very remarkable anticancer effect for C6 glioma cells.

3.3. Targeting effect in vitro

The cell inhibitory effect of C6 cells treatment with ANG-Rg3-NP was stronger than that treatment with ginsenoside-Rg3 and Rg3-NP (Figure 9). It was demonstrated that the ANG-Rg3-NP nanoparticles crossed the blood-brain barrier more easier and exhibited stronger inhibitory effect against C6 cells. Otherwise, the inhibitory effect of ANG-Rg3-NP was reduced by the addition of Angiopep-2. Because Angiopep-2 was the specific ligand of LRP-1, it was speculated that free Angiopep-2 competed with ANG-Rg3-NP for LRP-1 existed in BMEC and C6 cells, less nanoparticles entered to C6 cells and the inhibition was decreased, which indicated that the dual-targeting effect of ANG-Rg3-NP was related to LRP-1 receptors.

3.4. Cellular uptake on C6 cells

The results showed that there was a concentration-dependent uptake profile in C6 cells treated with ANG-coumarin-6-NP and coumarin-6-NP (Figure 10). Moreover, the fluorescence intensity of C6 cells treated with ANG-coumarin-6-NP were obviously higher than that of C6 cells treated with coumarin-6-NP at the concentration of coumarin-6 ranging from 10 μg/mL to 50 μg/mL (Figure 11). Also, for the time-dependent experiments, ANG-coumarin-6-NP exhibited stronger fluorescence intensity when compared with coumarin-6-NP at each time point ranging from 0.5 h to 4 h (Figure 12). What's more, the cellular uptake of ANG-coumarin-6-NP was significantly inhibited by free Angiopep-2. This could be explained by the fact that Angiopep-2 can compete with ANG-coumarin-6-NP for LRP receptor, which indicated that Angiopep-2 accelerated nanoparticles were efficiently internalized into C6 cells via receptor-mediated endocytosis.

4. Disscussion

Ginsenoside-Rg3 exhibited significant inhibitory effect on glioma cells, but the poor solubility and blood-brain barrier impermeability has limited the clinical application of ginsenoside-Rg3. The previous pharmacological studies of ginsenoside-Rg3 were mainly focused on the active pharmaceutical ingredients of

ginsenoside-Rg3. Thus, we combined the ginsenoside-Rg3 with nanoparticles and modified them with Angiopep-2 to construct the targeted delivery system to investigated their therapeutic effects on C6 glioma cells. The preparation process of nanoparticles is simple and has excellent physicochemical properties.

As expected, ginsenoside-Rg3 was successfully entrapped in the hydrophobic core of nanoparticles prepared with PEG-PCL. In tumor drug delivery, the size of nanoparticles needed to be perfectly controlled under 150 nm to meet the demand of EPR effect and decrease blood clearance (Alexis et al. 2008). In our study, the size of PEG-PCL nanoparticle was increased from 135.6±4.2 nm to 147.1±2.7 nm after being modified with Angiopep-2 so their size distribution was suitable for anti-tumor drug delivery. The existence of Angiopep-2 on the surface of Rg3-NP was confirmed by the elevation of zeta potential from -28.5±2.5 mV to -14.6±3.2 mV and this was mainly due to the electropositivity of the Angiopep-2 peptide. Futhermore, it was verified by BCA protein quantitation kit which the conjugation efficiency of Angiopep-2 was 39.5±0.9% when the molar ratio of PCL-PEG-MAL to Angiopep-2 was 1:1. The *in vitro* release results suggest that the moderate modification of Angiopep-2 do not evidently influence the *in vitro* release behavior of Rg3-NP (Figure 7).

In vitro cell experiments were performed on C6 glioma cells, as C6 cells were very close to human multiform glioblastoma by morphology, characteristics of invasive growth and spectrum of expressed proteins (Chekhonin et al. 2008). The cytotoxicity study confirmed that ANG-Rg3-NP exhibited stronger inhibitory effect to the proliferation of C6 cells than Rg3-NP and free ginsenoside-Rg3 (Figure 8), indicating that enhanced internalization of nanoparticles after functionalized with Angiopep-2 led to much higher ginsenoside-Rg3 concentration in C6 cells and thus more efficient anti-cancer activity. Cellular uptake results showed that a concentration-dependent and time-dependent fluorescence intensity of Angiopep-2 modified nanoparticles was achieved on C6 cells. Qualitative (Figure 10) and quantitative results (Figure 11, 12) exhibited a significantly higher fluorescence intensity on C6 cells treated with Angiopep-2 modified nanoparticles when compared

with that of unmodified nanoparticles. Furthermore, free Angiopep-2 significantly suppressed the cellular uptake of Angiopep-2 modified nanoparticles. Taking these results together, the improved anti-proliferative and induced apoptosis ability as well as enhanced cellular uptake was attributed to the Angiopep-2 peptide, which could bond the receptor of LRP-1 specifically and then facilitated the internalization of the nanoparticles into C6 cells.

At present, the research on pharmacological action of ANG-Rg3-NP was only performed in C6 cell. Future planned research will be *in vivo* tests and animal study to clarify the target and mechanisms of ANG-Rg3-NP as well as identify the adverse reactions. Futhermore, the combination of ginsenoside-Rg3 and chemical agents can be used to enhance the therapeutic effect and reduce the toxicity of chemical agents. Also, the research about the pharmacological action of ginsenoside-Rg3 can provide theoretical evidence for the application of natural drugs and Chinese medicine.

5. Conclusion

We successfully developed a novel targeted drug-carrier for the therapy of glioma. A series of nano-sized nanoparticles based on biodegradable PCL-PEG were prepared with a narrow size distribution. The ANG-Rg3-NP had excellent performance features characterized by an ideal particle size, high loading capacity, and sustained release characteristics. In the *in vitro* cytotoxicity study, ANG-Rg3-NP exhibited stronger inhibitory effect to the proliferation of C6 cells compared with Rg3-NP and free ginsenoside-Rg3. Also, *in vitro* dual-targeting effects further verified that ANG-Rg3-NP could be efficiently transported across blood-brain barrier and be specifically accumulated in C6 cells. Furthermore, the modification of Angiopep-2 accelerated the uptake of nanoparticles in C6 cells.

Our study demonstrated that ANG-Rg3-NP was an effective non-invasive approach to facilitate the access of ginsenoside-Rg3 to C6 cells. The findings here offered robust evidence for the targeting therapeutic effects of glioma and might lead to a significant advancement in the application of ginsenoside-Rg3 for targeted

therapy of glioma.

6. Acknowledgements

This work was supported by National Natural Science Foundation of China (NO. 81260645), the Natural Science Foundation of Hebei Province (No. H2016208058) and Key Project of Science and Technology Research in University of Hebei Province (ZD 2016009).

7. Disclosure of interest

The authors have no other financial involvement with any organization and ensure that this article content has no conflict of interest.

8. References

Dizon DS, Krilov L, Cohen E, Gangadhar T, Ganz PA, Hensing TA, Hunger S, Krishnamurthi SS, Lassman AB, Markham MJ, et al. 2016. Clinical cancer advances 2016: annual report on progress against cancer from the american society of clinical oncology. J Clin Oncol. 34(9):987-1011.

Li BO, Meng C, Zhang X, Cong D, Gao X, Gao W, Ju D1, Hu S. 2016. Effect of photodynamic therapy combined with torasemide on the expression of matrix metalloproteinase 2 and sodium-potassium-chloride cotransporter 1 in rat peritumoral edema and glioma. Oncol Lett. 11(3):2084-2090.

Ong BY, Ranganath SH, Lee LY, Lu F, Lee HS, Sahinidis NV, Wang CH. 2009. Paclitaxel delivery from PLGA foams for controlled release in post-surgical chemotherapy against glioblastoma multiforme. Biomaterials. 30(18):3189-96.

Jain RK, di Tomaso E, Duda DG, Loeffler JS, Sorensen AG, Batchelor TT. 2007. Angiogenesis in brain tumours. Nat Rev Neurosci. 8(8):610-622.

Pardridge WM. 2003. Blood-brain barrier drug targeting: the future of brain drug development. Mol Interv. 3(2):90-105.

Kim YJ, Zhang D, Yang DC. 2015. Biosynthesis and biotechnological production of ginsenosides. Biotechnol Adv. 33(6):717-735.

Choi YJ, Lee HJ, Kang DW, Han IH, Choi BK, Cho WH. 2013. Ginsenoside Rg3 induces apoptosis in the U87MG human glioblastoma cell line through the MEK signaling pathway and reactive oxygen species. Oncol Rep. 30(3):1362-1370.

Sin S, Kim SY, Kim SS. 2012. Chronic treatment with ginsenoside Rg3 induces Akt-dependent senescence in human glioma cells. Int J Oncol. 41(5):1669-1674.

Sun C, Yu Y, Wang L, Wu B, Xia L, Feng F, Ling Z, Wang S. 2016. Additive antiangiogenesis effect of ginsenoside Rg3 with low-dose metronomic

temozolomide on ratglioma cells both in vivo and *in vitro*. J Exp Clin Cancer Res. 35(1):32-44.

Nomani A, Nosrati H, Manjili HK, Khesalpour L, Danafar H. 2017. Preparation and Characterization of Copolymeric Polymersomes for Protein Delivery. Drug Res (Stuttg). 67(8): 458-465.

Nosrati H, Adibtabar M, Sharafi A, Danafar H, Hamidreza Kheiri M. 2018. PAMAM-modified citric acid-coated magnetic nanoparticl biocompatible carrier against human breast cancer cells. Drug Dev Ind Pharm. 44(8):1377-1384.

Nosrati H, Mojtahedi A, Danafar H, Kheiri Manjili H. 2018. Enzymatic stimuli-responsive methotrexate-conjugated magnetic nanoparticles for target delivery to breast cancer cells and release study in lysosomal condition. J Biomed Mater Res A. 106(6): 1646-1654.

Nosrati H, Rashidi N, Danafar H, Manjili HK. 2017. Anticancer activity of tamoxifen loaded tyrosine decorated biocompatible Fe3O4 magnetic nanoparticles against breast cancer cell lines. J Inorg Organment P. 28(3):1178-1186.

Salehiabar M, Nosrati H, Davaran S, Danafar H, Manjili HK. 2018. Facile synthesis and characterization of L-aspartic acid coated iron oxide magnetic nanoparticles (IONPs) for biomedical applications. Drug Res (Stuttg). 68(5): 280-285.

Ashley CE, Carnes EC, Phillips GK, Padilla D, Durfee PN, Brown PA, Hanna TN, Liu J, Phillips B, Carter MB, et al. 2011. The targeted delivery of multicomponent cargos to cancer cells by nanoporous particle-supported lipid bilayers. Nat Mater. 10(5):389-397.

Deng C, Jiang Y, Cheng R. 2012. Biodegradable polymeric micelles for targeted and controlled anticancer drug delivery: promises, progress and prospects. Nano Today. 7(5):467-480.

Cabral H, Kataoka K. 2014. Progress of drug-loaded polymeric micelles into clinical

studies. J Control Release. 190:465-476.

Lin W. 2015. Introduction: nanoparticles in medicine. Chem Rev. 115(19):10407-10409.

Beduneau A, Saulnier P, Benoit JP. 2007. Active targeting of brain tumors using nanocarriers. Biomaterials. 28(33):4947-4967.

Xin H, Sha X, Jiang X, Zhang W, Chen L, Fang X. 2012. Anti-glioblastoma efficacy and safety of paclitaxel-loading Angiopep-conjugated dual targeting PEG-PCL nanoparticles. Biomaterials. 33(32):8167-8176.

Demeule M, Currie JC, Bertrand Y, Ché C, Nguyen T, Régina A, Gabathuler R, Castaigne JP, Béliveau R. 2008. Involvement of the low-density lipoprotein receptor-related protein in the transcytosis of the brain delivery vector angiopep-2. J Neurochem. 106(4):1534-1544.

Xin H, Jiang X, Gu J, Sha X, Chen L, Law K, Chen Y, Wang X, Jiang Y, Fang X. 2011. Angiopep-conjugated poly (ethylene glycol) -co-poly (e-caprolactone) nanoparticles as dual-targeting drug delivery system for brain glioma. Biomaterials. 32(18):4293-4305.

Liu Z, Jiang M, Kang T, Miao D, Gu G, Song Q, Yao L, Hu Q, Tu Y, Pang Z, et al. 2013. Lactoferrin-modified PEG-co-PCL nanoparticles for enhanced brain delivery of NAP peptide following intranasal administration. Biomaterials. 34(15):3870-3881.

Zhu Y, Zhang J, Meng F, Deng C, Cheng R, Feijen J, Zhong Z. 2016. cRGD-functionalized reduction-sensitive shell-sheddable biodegradable micelles mediate enhanced doxorubicin delivery to human glioma xenografts *in vivo*. J Control Release. 233:29-38.

Mohammadi G, Shakeri A, Fattahi A, Mohammadi P, Mikaeili A, Aliabadi A, Adibkia K. 2017. Preparation, physicochemical characterization and anti-fungal

evaluation of nystatin-loaded PLGA-glucosamine nanoparticles. Pharm Res. 34(2):301-309.

Hu Q, Gao X, Kang T, Feng X, Jiang D, Tu Y, Song Q, Yao L, Jiang X, Chen H, et al. 2013. CGKRK-modified nanoparticles for dual-targeting drug delivery to tumor cells and angiogenic blood vessels. Biomaterials. 34(37):9496-9508.

Salehiabar M, Nosrati H, Javani E, Aliakbarzadeh F, Kheiri MH, Davaran S, Danafar H. 2018. Production of biological nanoparticles from bovine serum albumin as controlled release carrier for curcumin delivery. Int J Biol Macromol. 115: 83-89.

Chen C, Duan Z, Yuan Y, Li R1, Pang L, Liang J, Xu X, Wang J. 2017. Peptide-22 and cyclic RGD functionalized liposomes for glioma targeting drug delivery overcoming BBB and BBTB. ACS Appl Mater Interfaces. 9(7):5864-5873.

Koo YE, Reddy GR, Bhojani M, Schneider R, Philbert MA, Rehemtulla A, Ross BD, Kopelman R. 2006. Brain cancer diagnosis and therapy with nanoplatforms. Adv Drug Deliv Rev. 58(14):1556-1577.

Arthur JM. 2000. The MDCK cell line is made upof populations of cells with diverse resistive andtransport properties. Tissue Cell. 32(5):446-450.

Gu G, Xia H, Hu Q, Liu Z, Jiang M, Kang T, Miao D, Tu Y, Pang Z, Song Q, et al. 2013. PEG-co-PCL nanoparticles modified with MMP-2/9 activatable low molecular weight protamine for enhanced targeted glioblastoma therapy. Biomaterials. 34(1):196-208.

Tang L, Yang X, Yin Q, Cai K, Wang H, Chaudhury I, Yao C, Zhou Q, Kwon M, Hartman JA, et al. 2014. Investigating the optimal size of anticancer nanomedicine. Proc Natl Acad Sci U S A. 111(43):15344-15349.

Li SD, Huang L. 2008. Pharmacokinetics and biodistribution of nanoparticles. Mol Pharm. 5(4):496-504.

Liu H, Gao M, Xu H, Guan X, Lv L, Deng S, Zhang C, Tian Y. 2016. A promising emodin-loaded poly (lactic-co-glycolic acid)-d- α -tocopheryl polyethylene glycol 1000 succinate nanoparticles for liver cancer therapy. Pharm Res. 33(1):217-236.

Torehilin VP. 2001. Structure and design of Polymeric surfactant-based drug delivery systems. J Control Release. 73(2-3):137-172.

Nosrati H, Adinehvand R, Manjili HK, Rostamizadeh K, Danafar H. 2018. Synthesis, characterization and kinetic release study of methotrexate loaded mPEG-PCL polymersomes for inhibition of MCF-7 breast cancer cell line. Pharm Dev Technol. 1-10.

Nosrati H, Salehiabar M, Davaran S, Danafar H, Manjili HK. 2017. Methotrexate-conjugated L-lysine coated iron oxide magnetic nanoparticles for inhibition of MCF-7 breast cancer cells, Drug Dev Ind Pharm. 44(6): 886-894.

Rostamizadeh K, Manafi M, Nosrati H, Manjilia HK, Danafa H. 2018. Methotrexate-conjugated mPEG-PCL copolymers: a novel approach for dual triggered drug delivery. New J Chem. 42: 5937-5945.

Benyettou F, Fahs H, Elkharrag R, Bilbeisi R, Asma B, Rezgui R. 2017. Selective growth inhibition of cancer cells with doxorubicin-loaded CB [7]-modified iron-oxide nanoparticles, RSC Adv. 7(38): 23827-23834.

Alexis F, Pridgen E, Molnar LK, Farokhzad OC. 2008. Factors affecting the clearance and biodistribution of polymeric nanoparticles. Mol Pharm. 5(4):505-515.

Chekhonin VP, Baklaushev VP, Yusubalieva GM, Pavlov KA, Ukhova OV, Gurina OI. 2007. Modeling and immunohistochemical analysis of C6 glioma *in vivo.* Bull Exp Biol Med. 143(4):501-509.

Figure 1

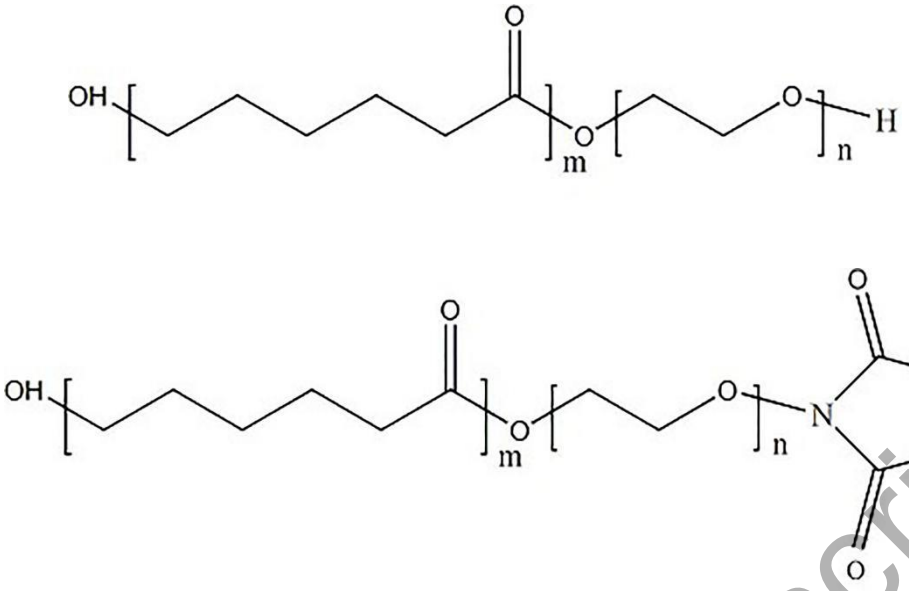

Figure 1. Chemical structures of PCL-PEG (A) and PCL-PEG-MAL (B).

Figure 2

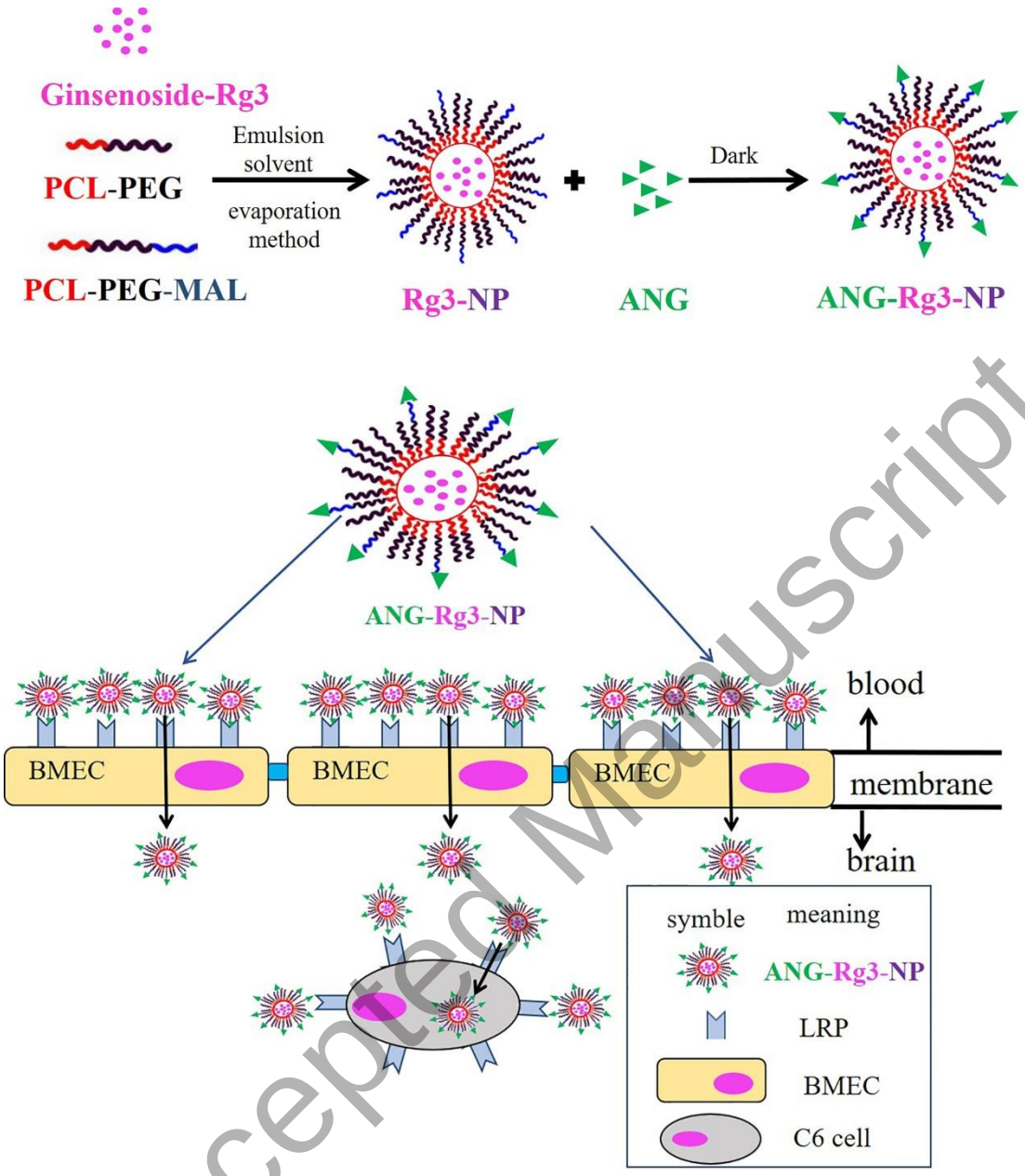

Figure 2. The preparation process of ANG-Rg3-NP and the nanoparticles acrossed blood brain barrier and C6 glioma cell.

Figure 3

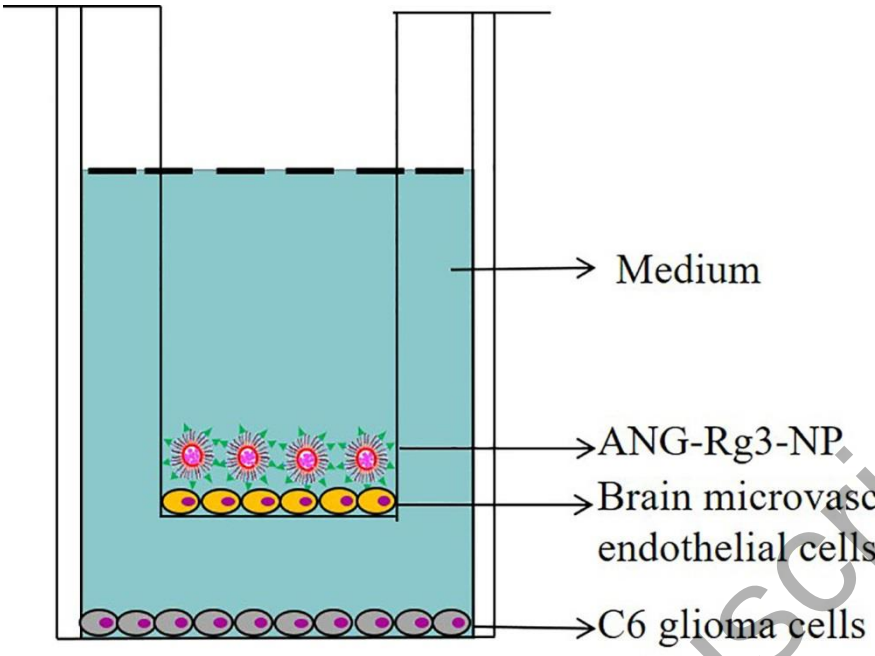

Figure 3. The co-culture model of BMEC-C6 cells.

Figure 4

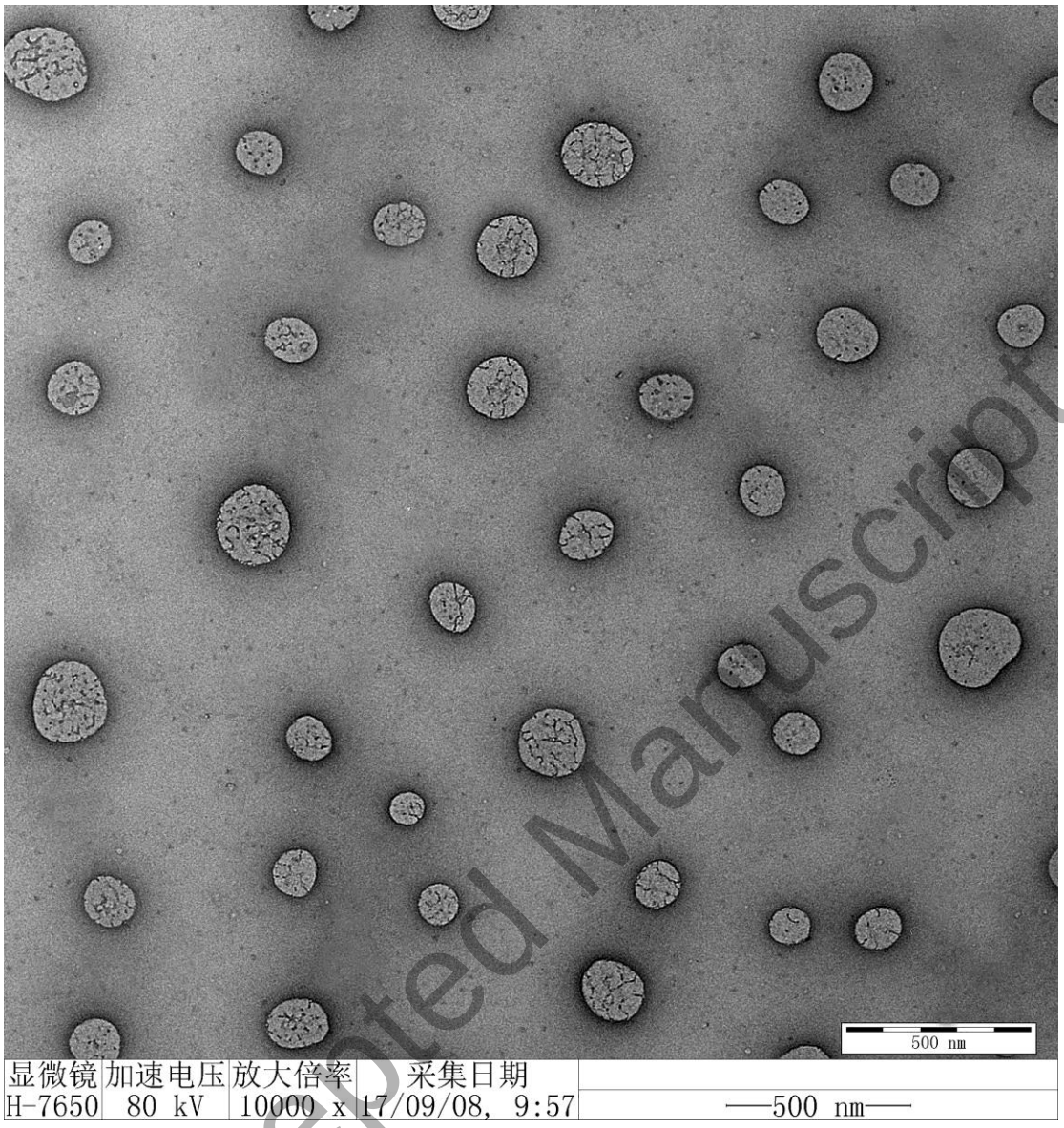

Figure 4. The TEM image of ANG-Rg3-NP after staining with 2% (w/v) phosphotungstic acid solution and drying at room temperature. Original magnification: 10000×. The bar is 500 nm.

Figure 5

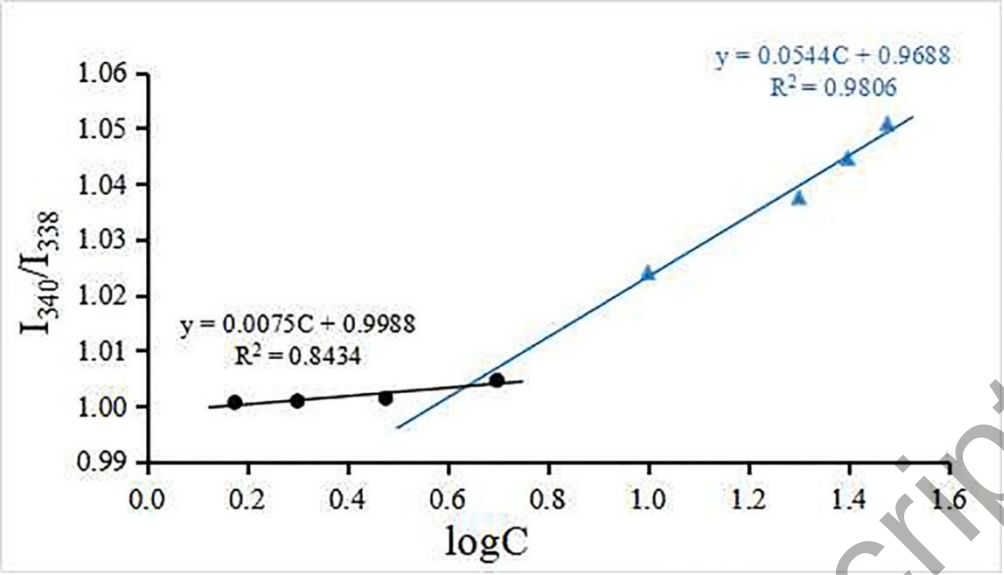

Figure 5. The critical micelle concentration of PCL-PEG. Data expressed as mean±SD (n=3).

Figure 6

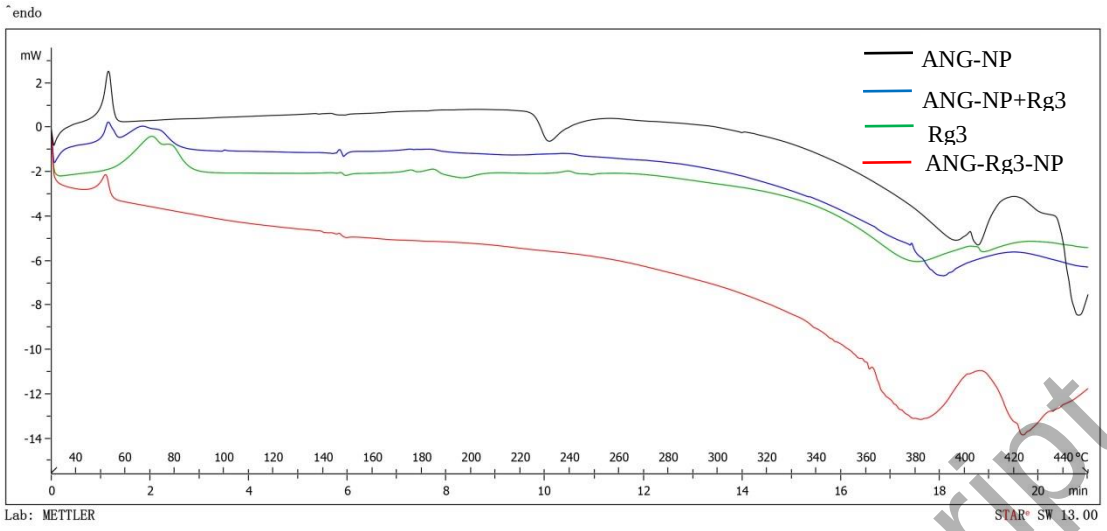

Figure 6. The thermograms of Rg3, ANG-NP, ANG-Rg3-NP as well as the physical mixture of Rg3 and ANG-NP.

Figure 7

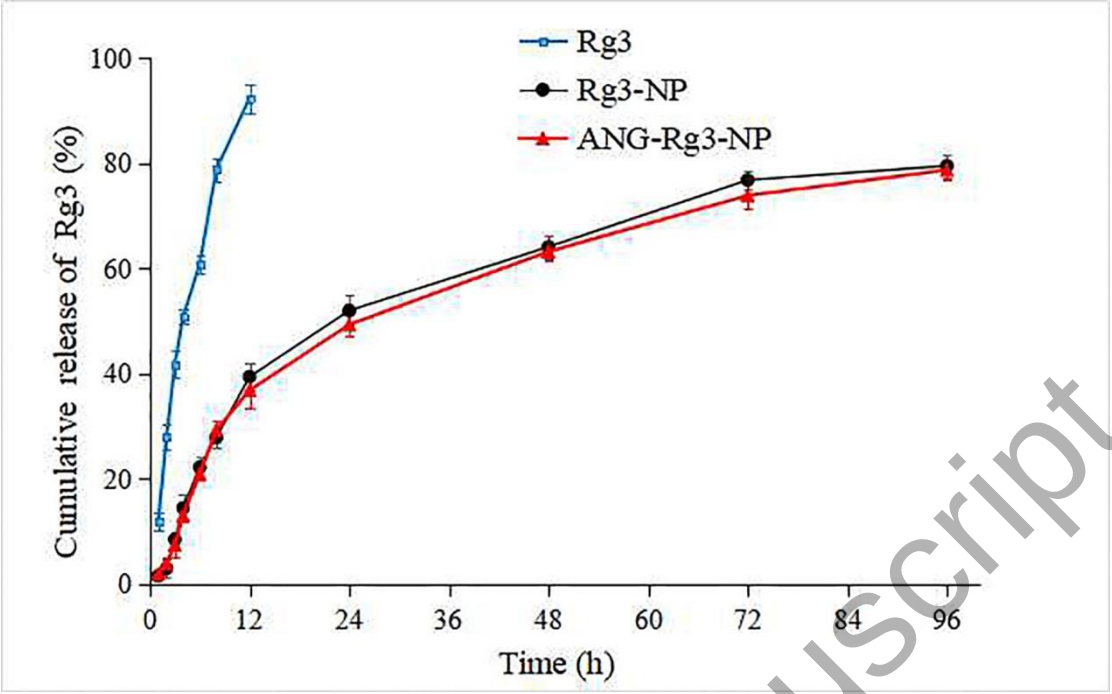

Figure 7. The cumulative release of Rg3-NP and ANG-Rg3-NP in saline with 1% Tween-80(n=3).

Figure 8

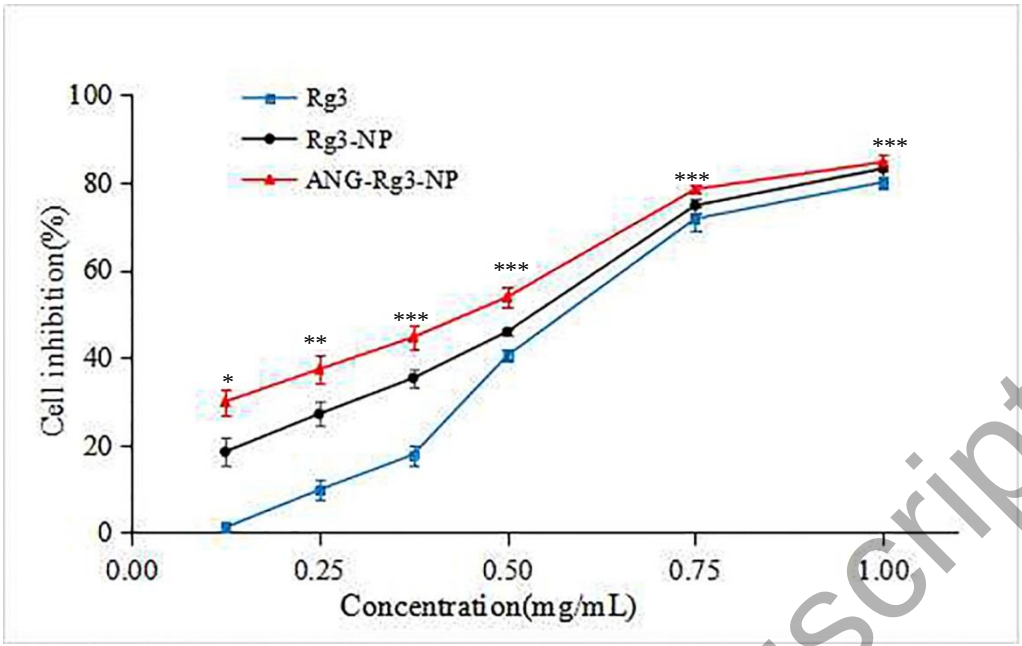

Figure 8. Cell inhibition of C6 cells after treated with Rg3, Rg3-NP and ANG-Rg3-NP for 48 h at 37℃(n=3). $^{*}P<0.05$, $^{**}P<0.01$, $^{***}P<0.001$, significantly different with the group of Rg3.

Figure 9

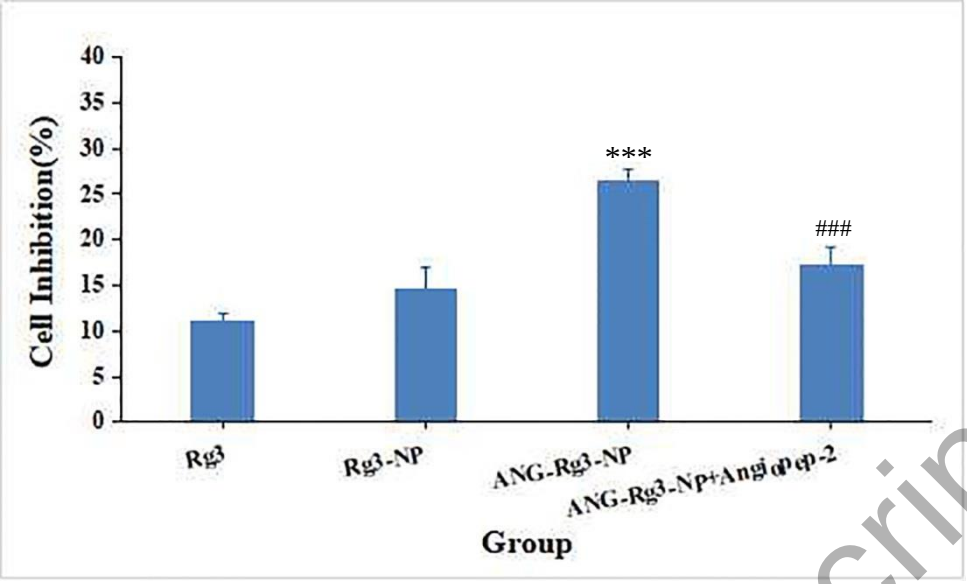

Figure 9. The targeting effect: cell inhibition of C6 cells after treated with Rg3, Rg3-NP, ANG-Rg3-NP and ANG-Rg3-NP+Angiopep-2 for 12 h at 37℃ (n=3). $^{***}P<0.001$ significantly different with the group of Rg3. $^{###}P<0.001$ significantly different with the group of ANG-Rg3-NP.

Figure 10

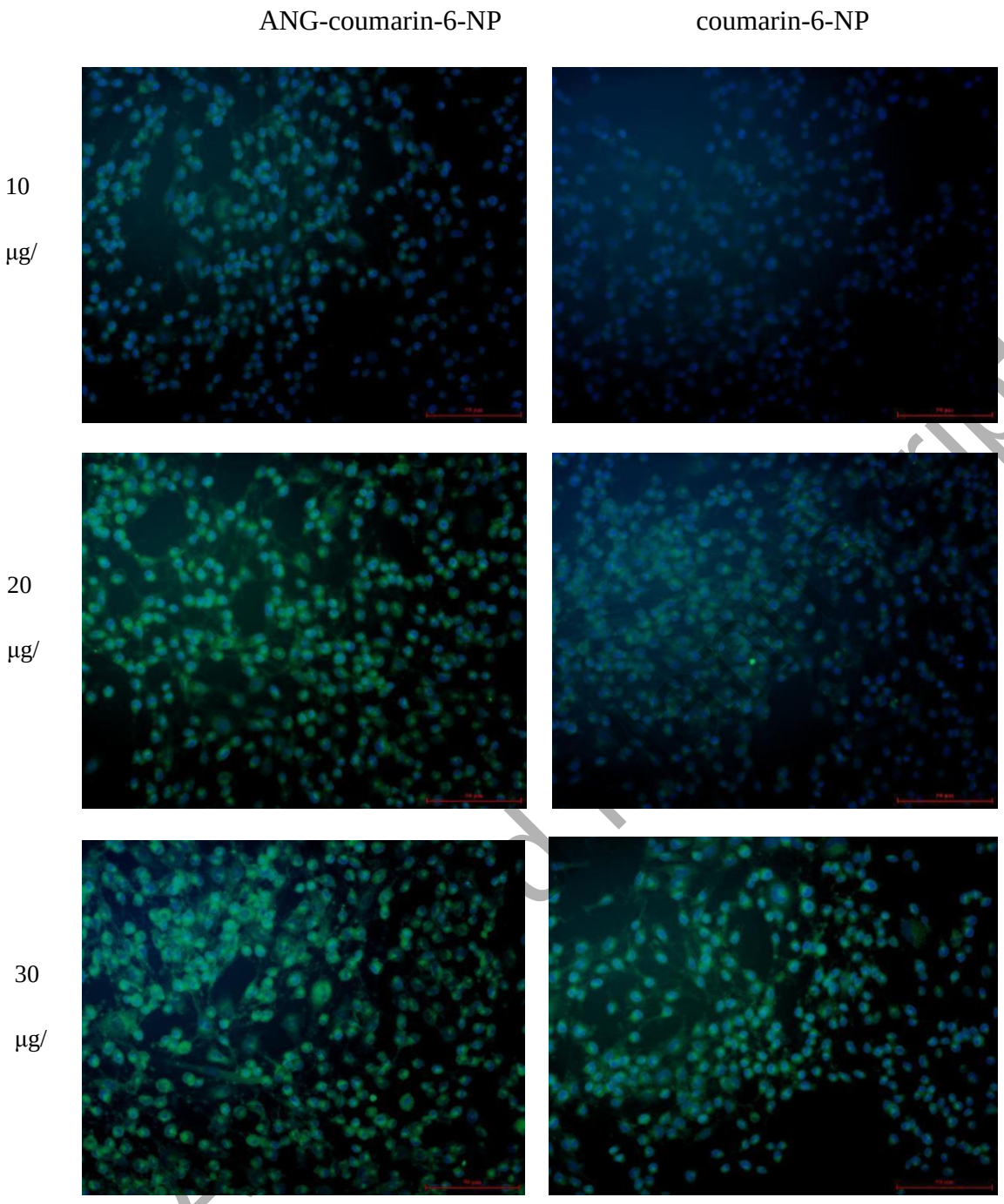

40 μg/

50 μg/

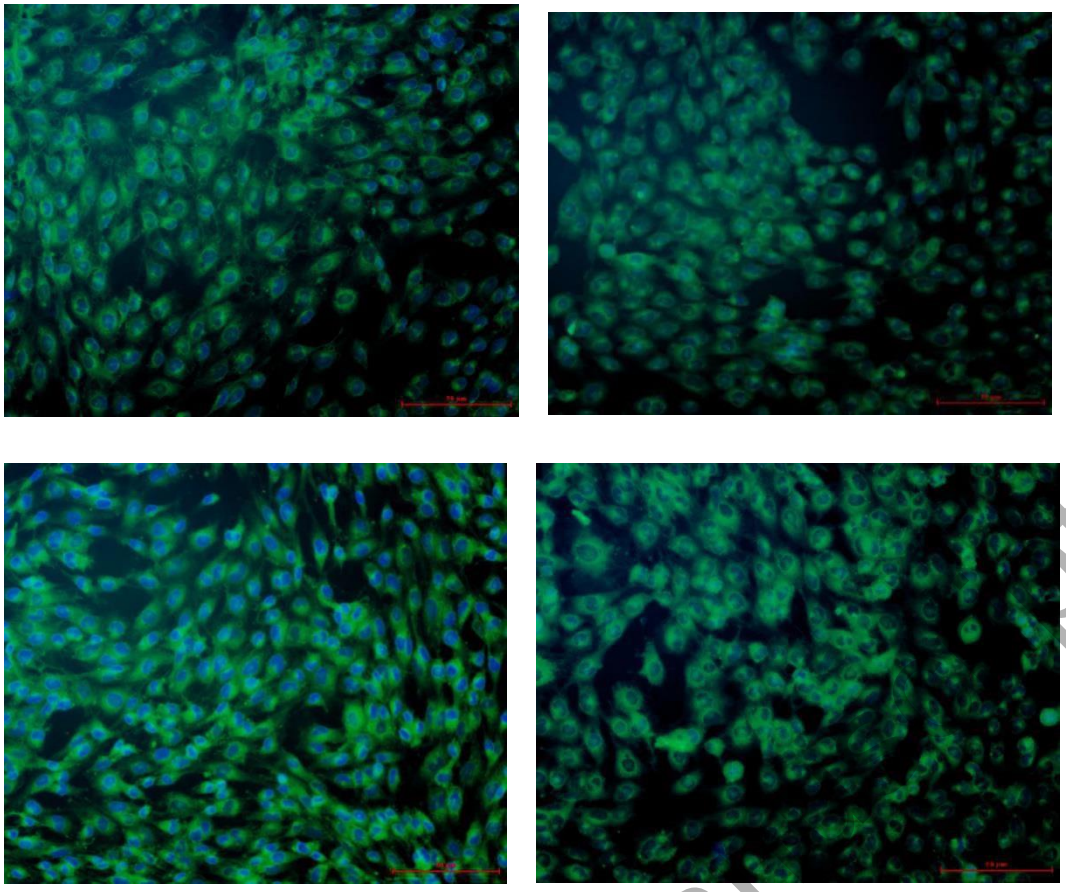

Figure 10. Celluar uptake of ANG-coumarin-6-NP and coumarin-6-NP in C6 cells after incubation for 1 h at the concentration of coumarin-6 ranging from 10 μg/mL to 50 μg/mL. Green, coumarin-6-loaded nanoparticles. Blue, cell nuclei stained with DAPI. Original magnification: 200×. The bar is 50μm.

Figure 11

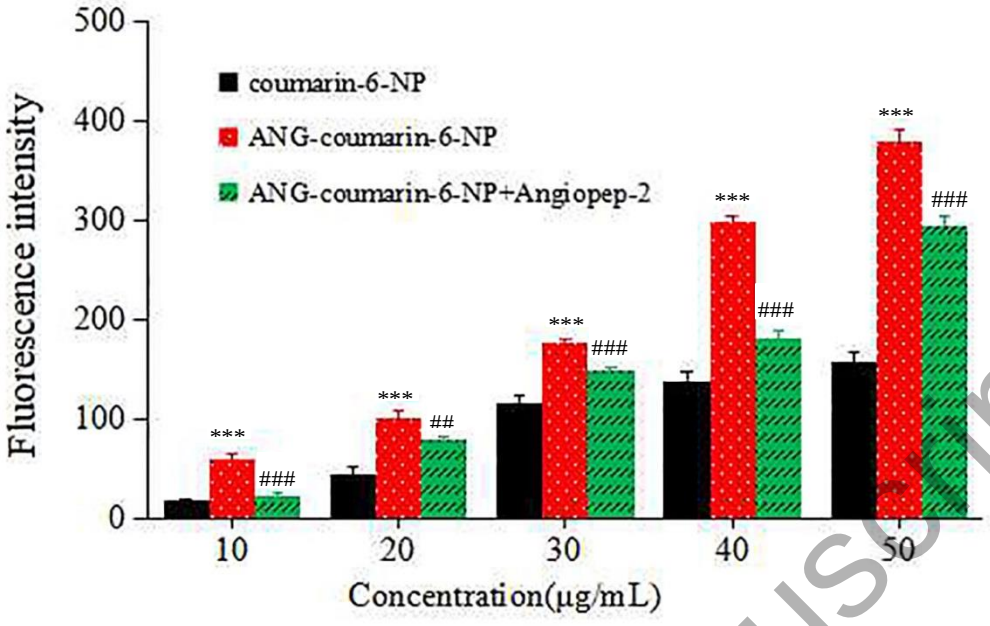

Figure 11. Celluar uptake of coumarin-6-NP, ANG-coumarin-6-NP and ANG-coumarin-6-NP+Angiopep-2 (10 μg/mL) in C6 cells after incubation for 2 h at the concentration of coumarin-6 ranging from 10 μg/mL to 50 μg/mL. $^{***}P<0.001$, significantly different with the group of coumarin-6-NP; $^{##}P<0.01$, $^{###}P<0.001$ significantly different with the group of ANG-coumarin-6-NP.

***

Figure 12

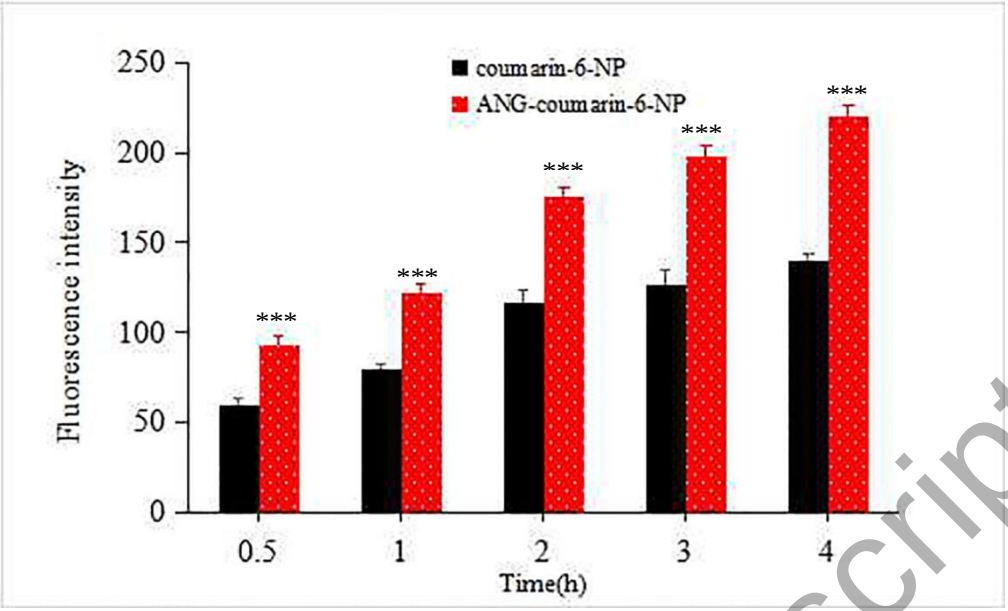

Figure 12. Celluar uptake of coumarin-6-NP and ANG-coumarin-6-NP at the concentration of coumarin-6 was 30 μg/mL and the incubation time ranging from 0.5 h to 4 h in C6 cells. $^{***}P<0.001$, significantly different with the group of coumarin-6-NP.